J. Fluid Mech. (1985), *vol.* 152, *pp.* 39–48
Printed in Great Britain

Convective motions in a spherical shell

By ABDELFATTAH ZEBIB, ATUL K. GOYAL
Department of Mechanical and Aerospace Engineering, Rutgers University, New Brunswick, NJ 08903

AND GERALD SCHUBERT
Department of Earth and Space Science, University of California, Los Angeles, CA 90024

(Received 1 March 1984 and in revised form 18 July 1984)

We compute the axisymmetric convective motions that exist in a spherical shell heated from below with inner to outer radius ratio equal to 0.5. The boundaries are stress-free and gravity is directly proportional to radius. Accurate solutions at large Rayleigh numbers ($O(10^5)$) are made feasible by a spectral method that employs diagonal-mode truncation. By examining the stability of axisymmetric motions we conclude that the preferred form of convection varies dramatically according to the value of the Rayleigh number. While axisymmetric motions with different patterns may exist for modestly nonlinear convection, only a single motion persists at sufficiently large values of the Rayleigh number. This circulation is symmetric about the equator and has two meridional cells with rising motion at the poles. Instability of this single axisymmetric motion determines that the preferred pattern of three-dimensional convection has one azimuthal wave.

1. Introduction

Nonlinear thermal convection in spherical shells has been studied extensively in the past few years. Busse (1975) and Busse & Riahi (1982) have considered the problem of bifurcation from the conduction state due to spherically symmetric gravitation and heating. They show how the degeneracy of the linear problem (Chandrasekhar 1961) is reduced due to nonlinear selection. Thus instead of the $2l+1$ solutions of the linearized equations where l is the degree of the spherical harmonic, there are only about l nonlinearly admissible solutions. The preferred convective motion among these solutions can then be determined by linear stability methods. Such analyses by Busse and Busse & Riahi have led to results valid for values of the Rayleigh number Ra close to the eigenvalue of the linear problem that corresponds to l. In particular, the behaviour near the critical Rayleigh number Ra_{cr} is completely predicted, provided that the eigenvalue corresponding to l is a simple eigenvalue and is sufficiently smaller in value than the nearest eigenvalue corresponding to a different l. These analyses are applicable to any spherical symmetry-breaking bifurcation. Riahi, Geiger & Busse (1982) give results for thermal convection in shells of different size and mode of heating.

Because of its geophysical applications, axisymmetric convective motions due to different styles of heating in spherical shells of various sizes, including the sphere, have been computed for values of Ra about ten times Ra_{cr} (Hsui, Turcotte & Torrence 1972; Young 1974; Weir 1976, 1978; Zebib, Schubert & Straus 1980; Schubert & Zebib 1980; Zebib *et al.* 1983). Owing to the high degree of spherical symmetry in the mathematical models there are, *a priori*, two sets of possible nonlinear solutions.

One exhibits hemispherical symmetry and is composed of spherical harmonics of even degree l. The other contains both odd and even degree spherical harmonics and is not hemispherically symmetric. If the critical motion corresponds to an even l, the only steady, axisymmetric solutions are a pair of equatorially symmetric motions with opposite senses of rotation. Except in the special case when the linear operator is self-adjoint, this pair of motions represents a transcritical bifurcation (Busse 1975; Busse & Riahi 1982). If the critical motion is an odd l, convection sets in as a supercritical bifurcation, with the subsequent axisymmetric steady state dominated by an odd number of cells equal to the critical l. A pair of hemispherical solutions also exists for values of Ra greater than the smallest linear eigenvalue corresponding to an even l; the motion is dominated by a number of cells equal to this even l (Zebib *et al.* 1983). The steady solutions with odd numbers of cells cease to exist after some modest supercritical Ra (Zebib *et al.* 1983).

The case of a shell with inner to outer radius ratio η equal to 0.5 is important in modelling mantle convection in the Earth (Schubert 1979). When such a shell, with stress-free boundaries and gravitational acceleration proportional to radial position, is heated from below, the first three eigenvalues (in increasing order) of the linear problem are 978.5 for $l = 3$, 1095.7 for $l = 2$, and 1109.6 for $l = 4$. The three-cell motion begins at $Ra = 978.5$ and ceases to exist at $Ra \approx 3300$ (Ra is based on the thickness of the shell, the temperature difference across it, and the acceleration of gravity at the outer radius). The hemispherical motions first occur at Ra about 1095.7 as $l = 2$ nonlinear circulations (the motion with downwelling at the poles is subcritical). As Ra increases they quickly evolve into $l = 4$ circulations. The hemispherical flows are unstable to axisymmetric perturbations including odd-l contributions (Zebib *et al.* 1983).

In this paper we focus on the nature of convection (in the shell described above) at more geophysically relevant values of Ra (about $1000Ra_{\mathrm{cr}}$). A complete investigation of deep mantle convection should include three-dimensional effects as well as realistic rheologies (temperature-, pressure- and stress-dependent viscosity). Such a task must be entirely dependent on extensive numerical computations. Here we present a fundamental study of high-Rayleigh-number axisymmetric convection for Rayleigh numbers reaching to geophysically relevant values. The stability properties of these axisymmetric solutions determine the preferred pattern of convection including the form that fully three-dimensional motions are likely to take. The spectral method with full-mode truncation used by Zebib *et al.* (1980) is adequate for computation at Ra up to about $10Ra_{\mathrm{cr}}$. Here we employ diagonal-mode truncation (cf. Denny & Clever 1973), which enables us to compute accurate axisymmetric hemispherical convection at Ra as high as $100Ra_{\mathrm{cr}}$.

The major conclusion of the present work is that the only high-Ra axisymmetric convection in the shell is an $l = 2$ hemispherical motion with fluid rising at the pole. This indeed is a surprising result, since the two-cell circulations that set in at about Ra_{cr} ($l = 2$) do not exist beyond Ra slightly greater than Ra_{cr} ($l = 4$). However, we find that with increasing Ra the two-cell motions reappear. Other equatorially symmetric motions become unstable to general axisymmetric disturbances at relatively low Ra, and eventually cease to exist. Linear stability analysis indicates that the $l = 2$ motion which persists to high Ra is stable to three-dimensional perturbations with zonal wavenumbers greater than one, but is unstable to disturbances with a single azimuthal wave. Thus, although other three-dimensional motions which do not branch from axisymmetric steady states are possible, the

three-dimensional motion with a pair of meridional cells and one zonal wave, with polar upwelling, seems to be the preferred form of convection at high Ra. This result contrasts with the finding (Zebib *et al.* 1980) that the preferred form of convection near Ra_{cr} is a three-dimensional motion with three meridional cells and three azimuthal waves (which agrees with Busse & Riahi's (1982) conclusion that the motion is indeed three-dimensional at the onset of convection).

We look closely at the disappearance of $l = 2$ convection at slightly supercritical Ra and its reappearance at higher Ra. The competition between the $l = 2$ and the $l = 4$ motions near the onset of convection due to the proximity of their respective Ra_{cr} results in a complex configuration of stable and unstable branches of these solutions. A bifurcation diagram for hemispherical convection consistent with all the computational evidence is presented.

2. Mathematical model

The motion is referred to spherical coordinates (r, θ, ϕ). With the assumption of an infinite Prandtl number and a Boussinesq fluid, the incompressible Navier–Stokes and energy equations can be reduced to (Chandrasekhar 1961)

$$\nabla^4\left(\frac{\mathrm{L}^2\Phi}{r}\right) = (1-\eta)\,Ra\,\mathrm{L}^2\Theta, \tag{2.1}$$

$$\partial_t\Theta + (\boldsymbol{v}\cdot\nabla)(\Theta+\Theta_c) = \nabla^2\Theta, \tag{2.2}$$

where the operator L^2 is defined by

$$\mathrm{L}^2\Theta = -\frac{\partial_\theta(\sin\theta\,\partial_\theta\Theta)}{\sin\theta} - \frac{\partial^2_{\phi\phi}\Theta}{\sin^2\theta}, \tag{2.3}$$

and $\boldsymbol{v}$ is given in terms of the poloidal scalar $\Phi(r,t)$ according to

$$\boldsymbol{v} = \left(\frac{\mathrm{L}^2\Phi}{r^2}, \frac{\partial^2_{r\theta}\Phi}{r}, \frac{\partial^2_{r\phi}\Phi}{r\sin\theta}\right). \tag{2.4}$$

Here length, velocity and temperature are dimensionless with respect to $d = R_2 - R_1$, κ/d and $\Delta T = T_1 - T_2$ respectively, where R_1, R_2 and T_1, T_2 are the inner and outer radii and temperatures, and κ is the thermal diffusivity. $\Theta(r,t)$ is the temperature deviation from the basic conduction profile $\theta_c(r)$

$$\Theta_c = \frac{r_1 r_2}{r} - r_1, \tag{2.5}$$

$$r_1 = \frac{\eta}{1-\eta}; \quad r_2 = \frac{1}{1-\eta}; \quad \eta = \frac{R_1}{R_2}. \tag{2.6}$$

The Rayleigh number Ra is defined by

$$Ra = \frac{\alpha g_2 \Delta T d^3}{\nu\kappa}, \tag{2.7}$$

where α is the coefficient of thermal expansion, g_2 is the value of the gravitional acceleration (which is assumed to increase linearly with r) at R_2, and ν is the kinematic viscosity.

The boundary conditions corresponding to isothermal, stress-free inner and outer surfaces are

$$\Theta = v_r = \partial_{rr}^2 (rv_r) = 0 \quad \text{at } r_1, r_2. \tag{2.8}$$

Because the operators ∇ and L^2 are singular at $\theta = 0, \pi$, representations of Θ and Φ are sought in terms of non-singular Legendre functions of θ.

3. Spectral method

Solutions of (2.1) and (2.2) are constructed by assuming spectral representation for $\Theta(r,t)$ and $\Phi(r,t)$ which satisfy the homogeneous boundary conditions (2.8). In the full-mode truncation, these representations for axisymmetric convection are

$$\Theta(r,\theta,t) = \sum_{l=0}^{N_\theta} \sum_{j=1}^{N_r} \tau_{lj}(t) \sqrt{2} \sin j\pi(r-r_1) P_l(\cos\theta), \tag{3.1}$$

$$\Phi(r,\theta,t) = \sum_{l=0}^{N_\theta} \sum_{j=1}^{N_r} \tau_{lj}(t) f_{lj}(r) P_l(\cos\theta), \tag{3.2}$$

where P_l are normalized Legendre polynomials and N_r, N_θ are the truncation parameters. The radial functions $f_{lj}(r)$ are constructed such that the linear momentum equation (2.1) is satisfied term by term (Zebib *et al.* 1980).

With the diagonal-mode truncation the spectral representation is

$$\Theta(r,\theta,t) = \sum_{l=0}^{N} \sum_{j=1}^{N-l+1} \tau_{lj}(t) \sqrt{2} \sin j\pi(r-r_1) P_l(\cos\theta), \tag{3.3}$$

$$\Phi(r,\theta,t) = \sum_{l=0}^{N} \sum_{j=1}^{N-l+1} \tau_{lj}(t) f_{lj}(r) P_l(\cos\theta), \tag{3.4}$$

where N is the truncation parameter. If N_r, N_θ represent an accurate solution at some Ra then a more accurate solution is obtained with $N = \max(N_r, N_\theta + 1)$. The N_r, N_θ solution contains $(N_\theta + 1) N_r$ coefficients, while the N solution has only $\frac{1}{2}(N+1)(N+2)$ coefficients. With $N_r \approx N_\theta$, (3.1) contains approximately twice as many terms as (3.3). Thus for the same computer resources we obtain accurate solutions at higher Ra with diagonal truncation. For the equatorially symmetric solutions we take the truncation parameter N even, with a total of $(\frac{1}{2}N+1)^2$ spectral coefficients instead of the $\frac{1}{2}(N+1)(N+2)$ coefficients needed to represent a general axisymmetric solution.

The computational techniques for finding the steady states and testing for their instabilities all proceed in exactly the same manner as with full truncation. In particular, a Galerkin approach is used to derive the initial-value problem for τ_{lk}, $0 \leqslant l \leqslant N; 1 \leqslant k \leqslant N-l+1$:

$$\tau_{lk} = \sum_{j=1}^{N-l+1} L_{ljk} \tau_{lj} + \sum_{n,m=0}^{N} \sum_{i=1}^{N-n+1} \sum_{j=1}^{N-m+1} N_{lknimj} \tau_{ni} \tau_{mj}. \tag{3.5}$$

An important detail is the computer storage of the integrals L and N in (3.5) (which retain the same definition as in Zebib *et al.* 1980) arising from the radial inner products, since not all nonlinear interactions are needed in the diagonal truncation. We were able to devise a procedure in which only the necessary integrals are computed and stored. Thus, for the hemispherical solutions, computer storage of these quantities was about N^3, while the solutions with odd numbers of cells required about $3N^3$. Complete details may be found in Goyal (1982).

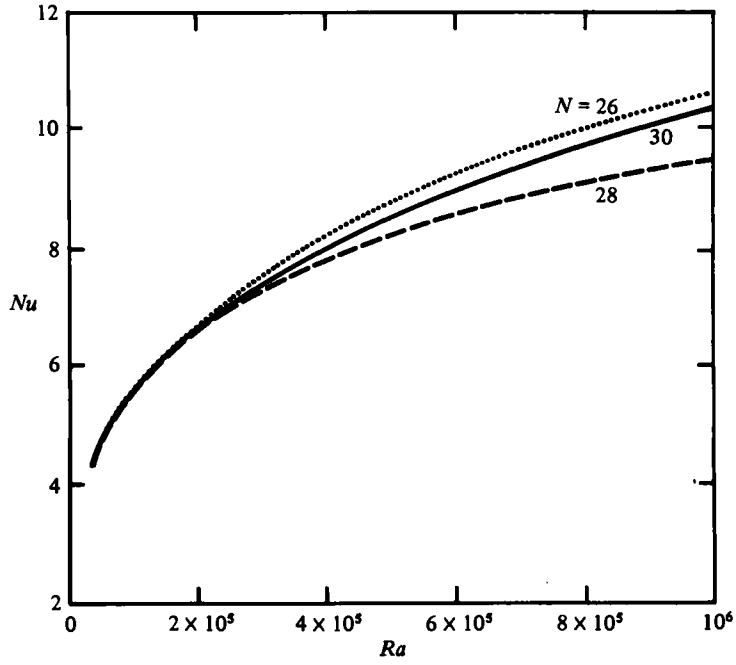

FIGURE 1. Variation of the Nusselt number Nu at the inner boundary with the Rayleigh number Ra for the 2-cell$^+$ motions for three values of the truncation parameter N. Accurate values of Nu are predicted with $N = 30$ up to $Ra \approx 200000$.

4. Results and discussion

We have found that there are 5 different axisymmetric steady convective motions in various ranges of Ra. We will refer to them according to the number of cells they contain. Comparison with previous full-mode truncation solutions (Zebib *et al.* 1983) confirms the accuracy of the diagonal-mode representation used here. The 3-cell motion begins at $Ra = 978.5$ and ceases to exist at $Ra \approx 3350$. This is confirmed from computations with N up to 20 (i.e. with 231 coefficients). The equatorially symmetric solutions are produced with N between 20 and 30; spot checks were made with $N = 34$. The 4-cell motions reported in Zebib *et al.* (1983) are extended here to the values of Ra where they cease to exist. The 4-cell$^+$ motion (i.e. with plumes at the poles) exists up to $Ra \approx 14500$. The 4-cell$^-$ solution with downwelling at the poles exists up to $Ra \approx 45000$. These 4-cell solutions are unstable to general axisymmetric as well as three-dimensional disturbances.

We first computed a 2-cell solution for $Ra \approx 100000$. This was accomplished via a fully implicit time-marching procedure. This solution, which is a 2-cell$^+$ motion, also exists for larger values of Ra up to at least 10^6! Figure 1 shows the Nusselt number (at the inner surface) variation with Ra for $N = 26$, 28 and 30. The Nusselt number is accurate to within 1% up to $Ra \approx 200000$ and to within 8.5% up to $Ra = 10^6$. We also computed the 2-cell$^+$ solutions at values of $Ra < 10^5$ and, as expected, these motions do not exist for Ra in a range between a value slightly greater than Ra_{cr} ($l = 4$) and about 2380. Since the 4-cell$^\pm$ motions began as 2-cell$^\mp$ convection at $Ra \approx 1095.7$ (Zebib *et al.* 1983), we also looked for a 2-cell$^-$ motion at sufficiently large Ra. The initial condition for the time-marching code was an artificial 2-cell motion with polar downwelling. We did compute the 2-cell$^-$ motion for $3630 \leqslant Ra \leqslant 135000$.

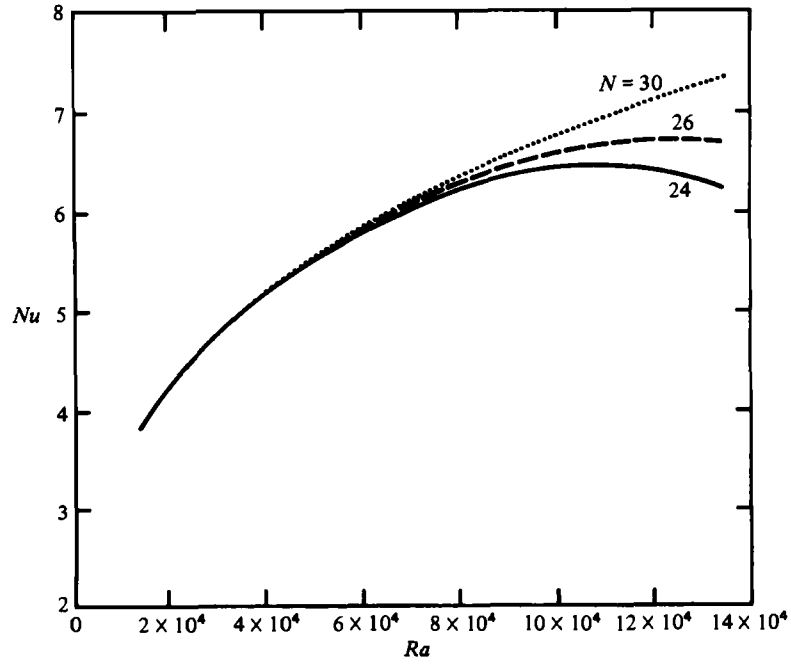

FIGURE 2. Same as figure 1, but for the 2-cell$^-$ solutions. Accurate Nusselt numbers are predicted at values of Ra less than about 60000 with $N = 30$.

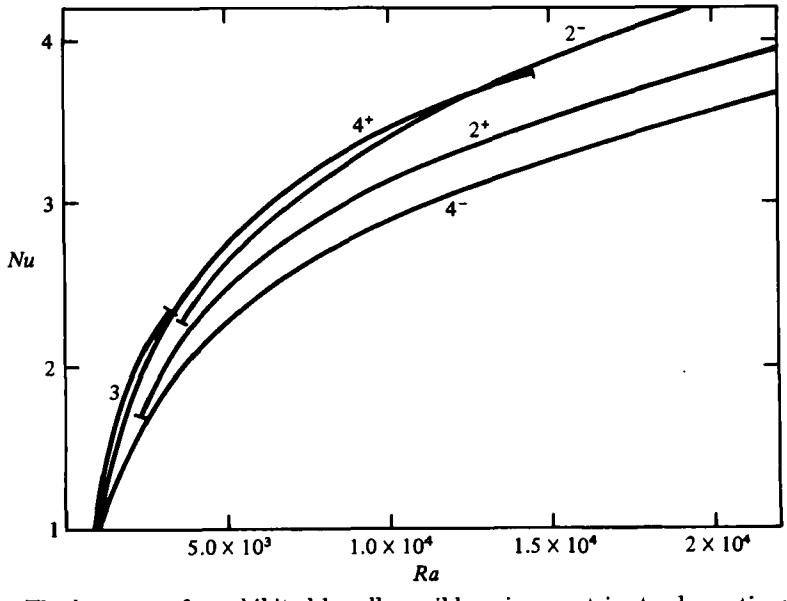

FIGURE 3. The heat transfer exhibited by all possible axisymmetric steady motions as a function of Ra. There is no 3-cell motion for $Ra > 3350$, no 2-cell$^-$ motion for $Ra > 135000$, no 4-cell$^+$ motion for $Ra > 14500$, and no 4-cell$^-$ solutions for $Ra > 45000$. The 4-cell$^\pm$ motions are secondary branches of a pair of 2-cell$^\mp$ motions which regain stability at Ra about 2380 and 3630 respectively. The 2-cell$^+$ motion is the only one of these axisymmetric solutions that exists at values of $Ra > 10^6$.

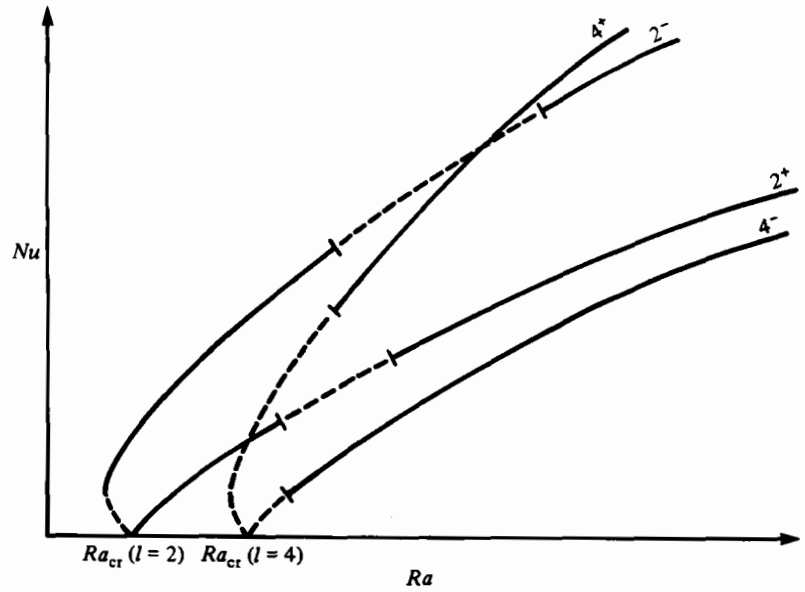

FIGURE 4. A sketch of the stable (solid) and unstable (dashed) hemispherical solutions in the (Nu, Ra)-plane. Both of the 2- and 4-cell motions represent transcritical bifurcations from the rest state. Secondary bifurcations, where the 2-cell$^{\pm}$ motions merge into 4-cell$^{\mp}$ convection through the appearance of polar cells (Zebib *et al.* 1983), occur at $Ra > Ra_{cr}$ ($l = 4$).

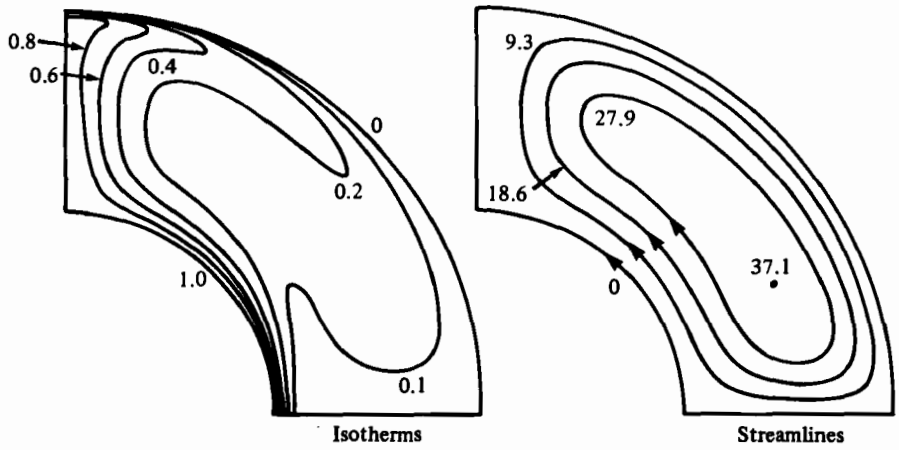

FIGURE 5. Streamlines and isotherms of the 2-cell^{+} convection at $Ra = 50000$ ($N = 30$). The thermal boundary layer structure is noticeable even at this relatively low Ra. The temperature is dimensionless with respect to the full temperature difference across the shell. The stream function is dimensionless with respect to thermal diffusivity.

The (Nu, Ra)-dependence of this solution is shown in figure 2 for $N = 24$, 26, 30; accurate Nu-values are obtained up to $Ra = 60000$.

Figure 3 summarizes the (Nu, Ra)-relationship in the Rayleigh-number range where the 5 axisymmetric solutions coexist. Because of scale the figure does not accurately reflect the solutions near $Nu = 1$. While the 3-cell solution transports more heat than any of the equatorially symmetric circulations, it only exists in a very limited range of supercritical Ra. The hemispherically symmetric motions with upwelling at the

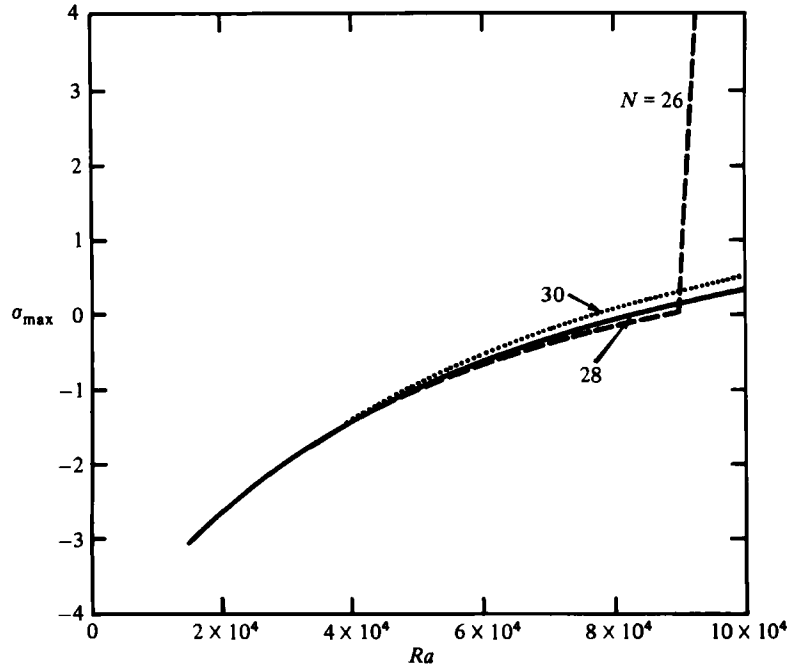

FIGURE 6. Variation with Ra of the maximum growth rate of an axisymmetric disturbance σ_{max} imposed on the 2-cell$^+$ motion. Growth rate is dimensionless with respect to shell thickness and thermal diffusivity. σ_{max} is sensitive to the truncation parameter N. Reliable determinations of σ_{max} extend to $Ra \approx 100000$ with $N = 30$. Instability of the 2-cell$^+$ convection occurs for $Ra \geqslant 80000$. The discontinuity of the slope in the case $N = 26$ indicates transition from real to complex eigenvalues.

equator transport more heat than their oppositely rotating counterparts. Two-cell convection is more vigorous than 4-cell convection when there is downwelling at the equator; the opposite is mostly true for upwelling at the equator. Convection with even numbers of cells extends to higher Ra when there is downwelling rather than upwelling at the equator.

Figure 4 is a sketch of the lower left corner of figure 3 magnified to reveal more detail. Only even-cell solutions are included. Certain features of this bifurcation diagram, described below, are not constrained by the calculations. The solid and dashed portions of the curves indicate regimes of existence and nonexistence of the solutions. The points Ra_{cr} ($l = 2$ and $l = 4$) are transcritical bifurcation points from the conduction state. The 2- and 4-cell solutions with rising motion at the equator set in as subcritical motions; with downwelling at the equator the circulations are supercritical. We are not absolutely certain that the Nusselt numbers decrease at the secondary bifurcation points involving transitions from two- to four-cell circulations (they could increase or suffer no discontinuities at transition). The points at which the 2-cell solutions regain their stability have been reasonably well defined by the computations. However, the corresponding points for the 4-cell solutions are not precisely located. An asymptotic analysis based on Rosenblat's (1979) method should lead to the analytic confirmation of figure 4 and the determination of the secondary bifurcation points and the points at which the 4-cell solutions regain stability.

The isotherms and streamlines of the 2-cell$^+$ motion at $Ra = 50000$ are shown in figure 5. The thermal boundary layer structure is evident even at this relatively

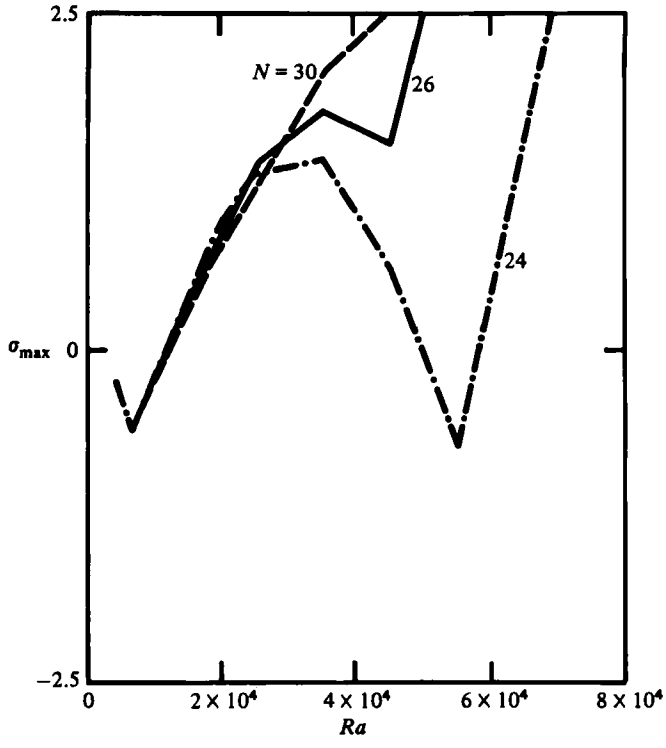

FIGURE 7. Same as figure 6 but for the 2-cell$^-$ motion. $N = 30$ is needed for reliable stability estimates at $Ra \lesssim 25000$. Instability is indicated for $Ra \geqslant 12000$.

low value of Ra. Although a boundary-layer transformation indicates that, as $Ra \to \infty$, $Nu = O(Ra^{\frac{1}{3}})$, a least-squares fit of the (Nu, Ra)-relationship (figure 1, $N = 30$) indicates that $Nu = O(Ra^{0.28})$ for $Ra \geqslant 500000$, while, for $Ra \geqslant 100000$, $Nu = O(Ra^{0.27})$. The thickening of the thermal boundary layer and plume at the pole is responsible for the decreased heat transfer at the inner surface.

The stability of the 2-cell$^{\pm}$ solutions to general axisymmetric disturbances is indicated by the maximum of the growth rates σ_{max} shown in figures 6 and 7. The growth rate is dimensionless with respect to thickness of the shell and the thermal diffusivity. For the purposes of predicting instability, the 2-cell$^+$ solutions are reliable up to $Ra \approx 100000$ with $N = 30$, while the 2-cell$^-$ motion is only reliable for $Ra \lesssim 25000$. The 2-cell$^-$ flows are stable for $Ra \leqslant 12000$, whereas the 2-cell$^+$ motions are stable up to $Ra \approx 80000$. Thus in the range $12000 \leqslant Ra \leqslant 80000$ the only steady axisymmetric motion is an equatorially symmetric 2-cell flow with upwelling at the poles. Furthermore, for $Ra \geqslant 80000$ there are no steady axisymmetric solutions. Analysis of the stability of the 2-cell$^+$ circulation to three-dimensional disturbances reveals that this solution is indeed unstable, but only to perturbations with one azimuthal wave. Thus the form of convection at sufficiently high Ra ($\geqslant 12000$) is a fully three-dimensional flow with one azimuthal wave, two meridional cells, and upwelling at the poles.

This research was supported by NASA through grants NSG 7601 and NSG 7315. The paper was written while A.Z. was a visitor at the Department of Chemical Engineering, Stanford University, and we are grateful to Dr G. M. Homsy for important discussions, for suggesting figure 4, and for his kind hospitality.

REFERENCES

BUSSE, F. H. 1975 Pattern of convection in spherical shells. *J. Fluid Mech.* **72**, 67–85.

BUSSE, F. H. & RIAHI, N. 1982 Pattern of convection in spherical shells. Part 2. *J. Fluid Mech.* **123**, 283–301.

CHANDRASEKHAR, S. 1961 *Hydrodynamic and Hydromagnetic Stability*. Clarendon.

DENNY, V. E. & CLEVER, R. M. 1973 Comparison of Galerkin's method and finite difference method for solving highly nonlinear thermally driven flows. *J. Comp. Phys.* **16**, 271–284.

GOYAL, A. K. 1982 High Rayleigh number thermal convection in spherical shells. Master's thesis, Rutgers University, New Brunswick, N.J.

HSUI, A. T., TURCOTTE, D. L. & TORRENCE, K. E. 1972 Finite amplitude thermal convection within a self-gravitating fluid sphere. *Geophys. Fluid Dyn.* **3**, 35–44.

RIAHI, N., GEIGER, G. & BUSSE, F. H. 1982 Finite Prandtl number convection in spherical shells. *Geophys. Astrophys. Fluid Dyn.* **20**, 307–318.

ROSENBLAT, S. 1979 Asymptotic methods for bifurcation and stability problems. *Stud. Appl. Maths* **60**, 241–259.

SCHUBERT, G. 1979 Subsolidus convection in the mantles of terrestial planets. *Ann. Rev. Earth Planet. Sci.* **7**, 289–342.

SCHUBERT, G. & ZEBIB, A. 1980 Thermal convection in an internally heated infinite Prandtl number fluid in a spherical shell. *Geophys. Astrophys. Fluid Dyn.* **15**, 65–90.

WEIR, A. D. 1976 Axisymmetric convection in a rotating sphere. Part 1. Stress-free surface. *J. Fluid Mech.* **75**, 49–79.

WEIR, A. D. 1978 Axisymmetric convection in a rotating sphere. Part 2. Non-slip surface. *Geophys. Astrophys. Fluid Dyn.* **11**, 205–222.

YOUNG, R. E. 1974 Finite-amplitude thermal convection in a spherical shell. *J. Fluid Mech.* **63**, 695–721.

ZEBIB, A., SCHUBERT, G. & STRAUS, J. M. 1980 Infinite Prandtl number thermal convection in a spherical shell. *J. Fluid Mech.* **97**, 257–277.

ZEBIB, A., SCHUBERT, G., DEIN, J. L. & PALIWAL, R. C. 1983 Character and stability of axisymmetric thermal convection in spheres and spherical shells. *Geophys. Astrophys. Fluid Dyn.* **23**, 1–42.